Journal of Taiwan Normal University: Mathematics, Science & Technology
2001, 46(1,2) , 13-22

Electronic-Structure Study of a Co-Al Alloy

[a]Li-Shing Hsu [b]S.-C. Chung [c]G.-H. Gweon

[a]Department of Physics, National Chang-Hua University of Education

[b]Synchrotron Radiation Research Center, Hsinchu 30077, Taiwan, Republic of China

[c]Randall Laboratory, University of Michigan, Ann Arbor, MI 48109-1120

Abstract

The electronic structure of a Co-Al alloy was studied by high-resolution x-ray photoemission spectroscopy, Bremsstrahlung isochromat spectroscopy, resonant photoemission spectroscopy, and x-ray-absorption spectroscopy (XAS) at the $L_{2,3}$ edges of Co. The asymmetry index of the Co 2p core levels for this Co-Al alloy is larger than that for Ni_3Al and for CoGa. This observation implies that the density of states at the Fermi level for this Co-Al alloy should be larger than that for Ni_3Al. The number of 3d holes per Co atom is 0.7 as determined from the XAS spectrum.

Keywords: Transition Metals and Alloys X-ray Absorption Spectra Photoemission Spectra

INTRODUCTION

Since Guillot *et al.* [1] discovered a resonantly enhanced valence-band (VB) satellite around the Ni 3p absorption threshold of elemental Ni, numerous resonant photoemission spectroscopic (RESPES) studies on transition metals and transition-metal compounds have been performed [2,3]. More recently, the electron-correlation effects in the Ni 3d bands of the Ni-Al [4-6], the Ni-Ga [5-10], and the Ni-In [5,8] intermetallic compounds were studied by using experimental techniques such as x-ray photoemission spectroscopy (XPS), Bremsstrahlung isochromat spectroscopy (BIS), RESPES at the Ni 3p or Ni 2p absorption edges, and x-ray absorption spectroscopy (XAS). The XPS and BIS spectra agree well with available density-of-states (DOS) curves derived from band-structure calculations. Only a partial filling of the empty Ni 3d states occurs on forming compounds with Al, Ga, or In. The DOS at the Fermi level (E_F) and the number of Ni 3d holes per Ni atom both decrease in the series: Ni_3Al, Ni_3In, Ni_3Ga, and NiGa. The so-called 6-eV photoemission satellite is observed in all these compounds and it is resonantly enhanced around the Ni 3p absorption edge, while around the Ni 2p absorption threshold it contributes much less weight to the photoemission spectra than the incoherent Auger process does. However, two controversial topics still exist in this field. The first is whether the resonantly enhanced photoemission satellite in Ni and Ni compounds is due to incoherent Auger or coherent process [11], while the second is whether the two-hole resonance exists in the VB photoemission spectra of 3d elements lighter than Ni (*e.g.* Fe and Co) [12]. Relatively speaking,

much less attention has been paid to the electronic structures of the Fe and Co compounds or alloys than to those of the Ni compounds or alloys. To fill this gap, an XPS study on the electronic structures of two Co-Ga intermetallic compounds and one Fe-Ga alloy has been reported [13]. No two-hole bound state was found in these materials. To our knowledge, no RESPES work at the Co 2p edges of Co metal and Co compounds or alloys has been reported, though RESPES studies at the Co 3p edges of some Co compounds do exist in the literature [14]. Technologically, the study of the magnetic, optical, and magneto-optical properties of some Co-Al alloy and multilayered films has recently been performed [15]. The purpose of this study is to use all of the above-mentioned experimental techniques to study the electronic structure of a Co-Al alloy and to address the above two controversial topics. The next section of this paper describes the experimental procedure. In section 3, the results are presented and discussed, and section 4 concludes this paper.

EXPERIMENTAL PROCEDURE

A Co-Al alloy was prepared by arc melting the weighted amounts of 99.9% pure Co and 99.999 pure Al (molar mass ratio of Co:Al=3:1) together under an argon atmosphere. It was then annealed in an evacuated (~10^{-6} Torr) quartz tube at 900℃ for 336 h to improve the homogeneity, and quenched into a water bath. The total loss of weight during these processes was 0.4%. The button was then cut and polished to obtain mirror-like surface. Powder x-ray diffractometry (XRD) showed that the sample composed of three phases: α -Co (fcc), β -CoAl (bcc), and α -Co_3Al (fcc). This is expected since α -Co_3Al is a high-temperature phase and will partially decompose into the other two phases below 800℃[16]. The XRD pattern of this Co-Al alloy is shown in Fig. 1, which shows that the sample composes of roughly 36% metallic Co, 28% CoAl, and 36% Co_3Al. Energy-dispersive x-ray (EDX) analysis showed that the molar ratio of Co:Al is 2.22:1. The residual resistivity (ρ) ratio ($\rho_{300K}/\rho_{4.2K}$) for this Co-Al alloy is only 1.4, while that for polycrystalline samples Fe_3Al and Ni_3Al is 2.3 and 4.5, respectively [17].

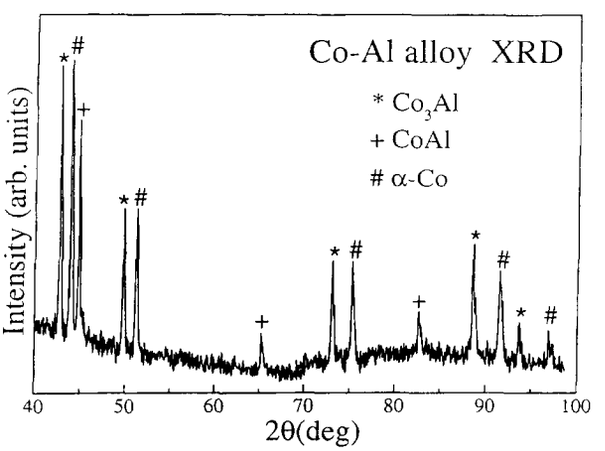

Fig. 1. XRD pattern for a Co-Al alloy.

The XPS and BIS spectra were measured in a Vacuum Generators ESCALAB, using the monochromatized Al K_α(1486.6 eV) radiation for XPS. The BIS spectrometer utilizes the same x-ray monochromator as the XPS system and, therefore, operates at the same photon energy. We checked the BIS spectra every 30 min and found no change of the shape of the spectra. This indicates that the electron damage to the sample surface is minimal. As a reference point for the binding energy (E_B), we used the Fermi edge of a sputter-cleaned silver sample measured under identical conditions. The energy resolutions are 0.64 and 0.9 eV for XPS and BIS, respectively, as determined from the clean silver XPS and BIS spectra. The probing depths for the XPS and BIS measurements are both about 20 Å. The pressure during the measurements was 1.5×10^{-10} Torr. The RESPES and XAS experiments were carried out on beam line B-15A at the Synchrotron Radiation Research Center, Hsinchu, Taiwan. Photon energies were selected with a high spherical grating monochromator, and a Vacuum Science Workshop 125-mm hemispherical analyzer was used in the fixed-analyzer-transmission mode to collect the RESPES and XAS spectra. The latter were collected by recording the total yield of secondary electrons from sample surface. The photon flux was obtained simultaneously by measuring the current of a Au mesh located near the exit slit of the monochromator and used for normalization of the RESPES and XAS spectra. The total energy resolution was 0.8 eV at $h\nu$ =780 eV and with analyzer pass energy of 20 eV. The probing depth for the RESPES and XAS measurements is roughly 15 Å and a few hundred Å, respectively. The RESPES and XAS spectra were recorded with the E vector of the x rays making 45° to the sample normal. This geometry would contribute roughly the same relative weight to the photoemission and to the Auger matrix elements [11]. The pressure during the measurements was 2×10^{-10} Torr.

The sample was cleaned by repeated cycles of sputtering with Ar ions and annealing to 500℃ until photoemission spectra showed no trace amount of O and C contamination on the sample surface. The sample surface after cyclic cleaning contained about twice more Al atoms than Co atoms, which was determined from the photoemission peak ratio of the Co 3p and Al 2p photoemission spectra at $h\nu$ = 777 eV after correcting for the photoionization cross sections [18]. Roughly the same surface segregation was found in the XPS spectrum. We note that this surface composition is very different from the bulk one as determined by EDX. Recent research [19] on surface segregation in the Ni-Al solid solution indicates that it depends on the annealing time and the annealing temperature, and anomalous increase in equilibrium segregation level becomes possible for temperatures above 650 ℃.

RESULTS AND DISCUSSION

Figure 2 shows XPS VB and BIS spectra for this Co-Al alloy. The XPS spectrum was first broadened by a Gaussian of 0.63 eV full width at half maximum to compensate for the worse energy resolution in the BIS measurement. The two spectra were then matched at E_F. The peak locates at E_B= 0.9 eV is due to Co 3d states. A second peak at E_B=1.2 eV due to d-like state of the Al atom is also resolved. The Co 3d peak was

observed at E_B~ 0.4 eV for elemental Co in an angle-resolved ultraviolet photoemission spectroscopic study [20]. The difference in E_B's of the Co 3d peaks for this Co-Al alloy and for Co metal is partially due to the worse energy resolution for XPS. Not much extra weight above background at E_B~ 4-6 eV is seen. Thus, the two-hole bound state is rather weak in this Co-Al alloy, if it exists. The BIS spectrum is dominated by a peak arising from antibonding state of Co 3d character at ~ 0.3 eV above E_F. We note that this peak lies ~ 0.5 eV above E_F for Co metal [21]. One can thus estimate the ferromagnetic exchange splitting of ~ 1.2 eV between the occupied spin-up and unoccupied spin-down states of this Co-Al alloy. The exchange splitting for Co metal is 0.93 $\pm$ 0.1 eV [21]. The exchange splitting is again overestimated partially due to the worse energy resolution employed in the present XPS and BIS measurements. A broad feature starting at ~ 5 eV above E_F is due to Al s-p states.

Figure 3 shows the Co 2p core-level spectrum for this Co-Al alloy. This spectrum was least-squares fitted with two Doniach-Sunjic line shape functions [22] for the Co $2p_{3/2}$ and $2p_{1/2}$ peaks. A Gaussian to simulate instrumental broadening and a Shirley-type background [23] were also included in the fitting process. The fitting result is shown as a solid line in Fig. 3. The E_B values for the Co 2p peaks thus obtained are listed in Table 1, along with the corresponding singularity index (α) as defined by the Doniach-Sunjic function. Also included in Table 1 are the corresponding values for CoGa and Ni_3Al. We note that the two-hole bound state observed in Ni metal and Ni compounds is rather weak in the Co 2p XPS spectrum of this Co-Al alloy, if it exists. Such state was not observed in the photoemission spectra of CoGa intermetallic compound and Fe-Ga alloy [13]. The chemical shifts of this Co-Al alloy with respect to elemental Co are very small, indicating very small charge transfer between Co and Al atoms. Small charge transfer of 0.283 from Al to Co in CoAl compound was

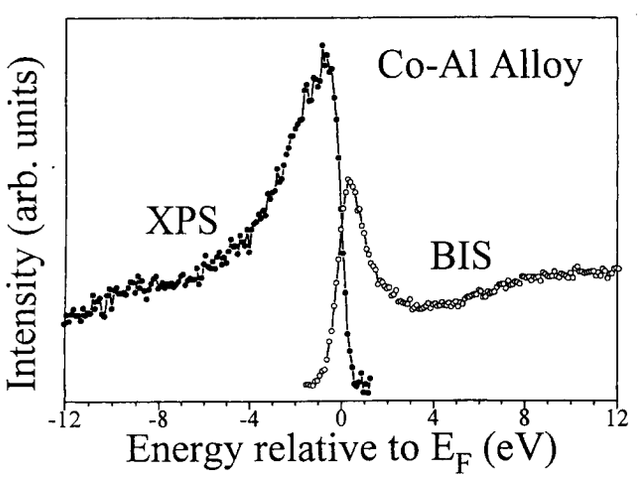

Fig. 2. XPS valence-band and BIS spectra for a Co-Al alloy. The line is to guide the eyes.

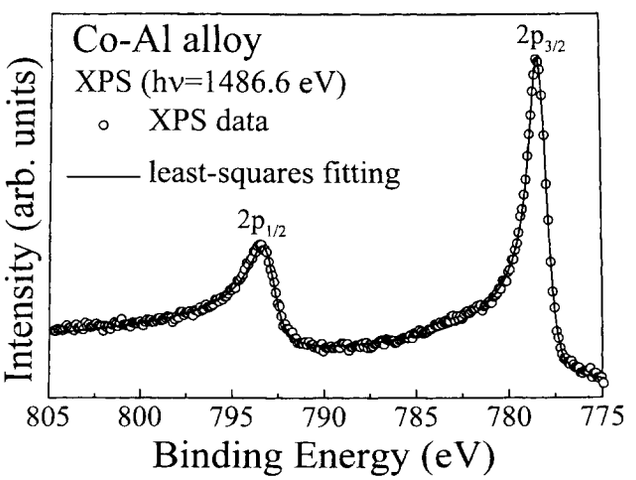

Fig. 3. XPS Co 2p photoemission spectrum for a Co-Al alloy. The line is a least-squares fitting of the XPS data.

Table 1. Binding energies (in eV), singularity index (α), and asymmetry index (α_i) of the transition-metal $2p_{3/2}$ and $2p_{1/2}$ levels for a Co-Al alloy, CoGa, and Ni_3Al.

	$E_B(2p_{3/2})$[a]	$(2p_{3/2})$	$E_B(2p_{1/2})$[a]	$\alpha_i(2p1/2)$	α_i[b]	$n(E_F)$[c]
Co-Al	778.2	0.33	793.0	0.48	2.52	(12.4, 9.2)
CoGa[d]	779.0	0.17	794.1	0.19	1.42	15
Ni_3Al[e]	852.8	0.25	869.9	0.28	1.75	(150,105)

[a] Uncertainty ± 0.1 eV.

[b] Average asymmetry index of the transition-metal $2p_{3/2}$ and $2p_{1/2}$ core levels.

[c] Density of states at the Fermi level in units of states/(Ry cell). For CoAl and Ni_3Al, the first and the second number in the parenthesis is the experimental and the theoretical value. The theoretical value for CoGa is obtained from Ref. [25].

[d] From Ref. [13].

[e] From Ref. [6].

reported previously [24]. The asymmetry index (α_i) is a function of α [22]. The average α_i value of the Co $2p_{3/2}$ and $2p_{1/2}$ levels for this Co-Al alloy calculated from the two α values is given in the sixth column in Table 1. Asymmetric core-level lines are generally observed in metals due to the response of the conduction electrons to the created photohole. The line asymmetry normally increases with an increasing local DOS at E_F ($n(E_F)$) value. The available experimental and theoretical $n(E_F)$ values for CoAl, CoGa, and Ni_3Al are listed in the last column in Table 1. The theoretical $n(E_F)$ values for CoAl and CoGa are from the band-structure calculations of Koch and Koenig [25]. The experimental $n(E_F)$ value for CoAl is from the specific-heat measurement of Begot et. al. [26] For Ni_3Al we chose the $n(E_F)$ value derived from the specific-heat measurement [27] neglecting electron-phonon interaction as the experimental one, and the band-calculated $n(E_F)$ value [28] as the theoretical one. They are enclosed in a parenthesis and separated by a comma in Table 1. It should be pointed out that higher experimental $n(E_F)$ values (175 [29], 178 [30], and 196 [30] states/(Ry cell)) derived from specific-heat measurements on Ni_3Al were reported. If one neglects the detailed band structures of this Co-Al alloy and Ni_3Al, the larger α_i value for this Co-Al alloy seems to suggest that the $n(E_F)$ value and the number of 3d holes per transition metal atom are both larger for this Co-Al alloy than for Ni_3Al.

Figure 4 shows the VB photoemission spectra of this Co-Al alloy at photon energies in the Co $2p_{3/2}$ range (772 to 783.3 eV), normalized to the photon

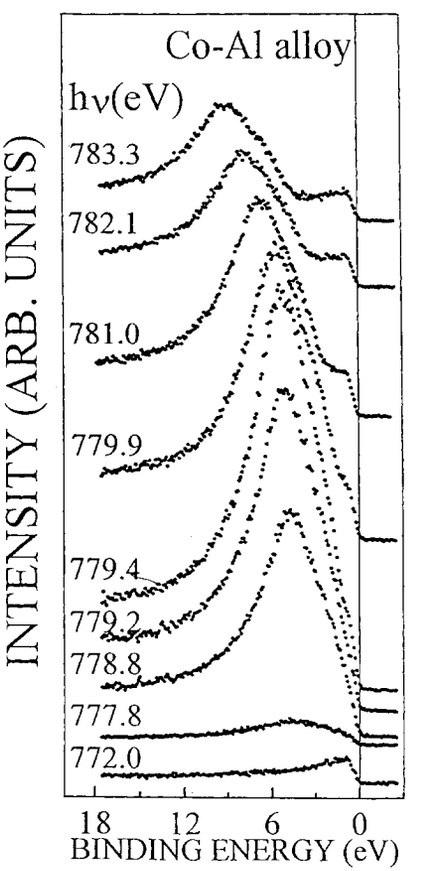

Fig. 4. RESPES spectra for a Co-Al alloy for various photon energies around the Co $2p_{3/2}$ absorption edge.

flux. The RESPES spectra are dominated by an Auger peak that appears at increasing E_B as the excitation energy increases. At the absorption maximum at 779.4 eV, the VB spectrum has its maximum at about 5 eV below E_F. In order to examine in more detail the VB photoemission intensity, we have measured the constant-initial-state (CIS) spectra. Such spectra are obtained by synchronously sweeping the photon energy with the transmission-energy window (about 1 eV wide) of the analyzer, so that E_B of the initial state is kept constant. Figure 5 displays two such CIS spectra, one for the initial state at 0.9 eV below E_F, the other for the initial state at 5 eV below E_F. These particular E_B's were chosen because the former represents the VB peak position, while the latter represents the peak position of the Auger emission. In addition to the strongly enhanced incoherent Auger emission the VB state at E_B=0.9 eV displays resonance behavior, even though the increase in intensity is much smaller than that of the Co $L_3M_{4,5}M_{4,5}$ Auger peak. This shows that the VB state has mainly Co 3d character. It has been shown [31] that the energy of the two-hole satellite on the Ni 3d band equals the difference in energy of the L_3 photoemission state and the $L_3M_{4,5}M_{4,5}$ Auger energy. If one applies this rule to the Co 3d state in this Co-Al alloy, one would get the two-hole satellite energy of 4.4 eV, which is larger than that (3.2 eV) obtained from Auger [32] and XPS [33] data of Co metal.

The XAS spectrum of this Co-Al alloy is displayed in Fig. 6. We note that there is one near-edge structure at 3.2 eV above the L_3 white line (779.4 eV), while no peak is observed above the L_2 white line (794.6 eV). The two white lines can be explained qualitatively by the multiplet structures and optical selection rules for transitions from a d^7 to the $2pd^8$ multiplets. The near-edge structure is due to transition to the Co 4s-like band, and has configuration

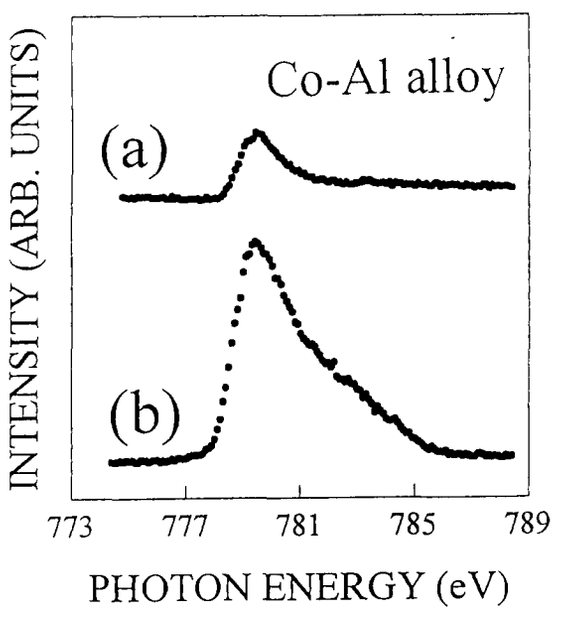

Fig. 5. Constant-initial-state spectra for a Co-Al alloy measured at a binding energy of (a) 0.9 eV and (b) 5 eV.

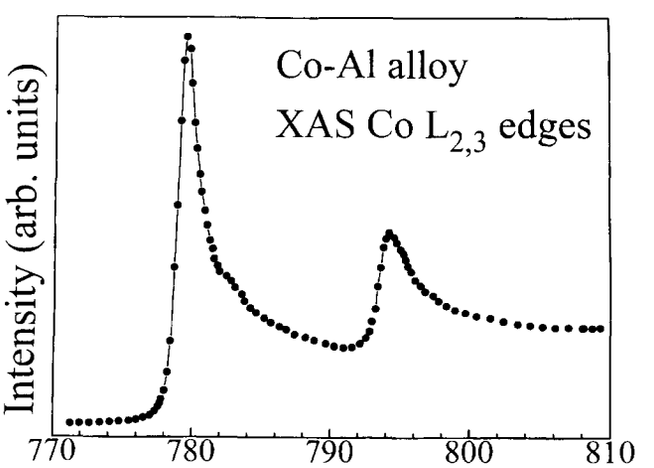

Fig. 6. XAS spectrum for a Co-Al alloy taken at the Co L_3 and L_2 edges. The line is to guide the eyes.

$2p_{3/2}$ $3d^9\underline{L}$. We note that since this Co-Al alloy has covalent bonding, the final-state levels with the same representation have interference. This can result in the deformation of the multiplet structures and the appearance of satellite structure. Thus, configuration mixing must be taken into account for a more complete analysis. The XAS energies are about 1.5 eV larger than those found in XPS. The difference in energy is caused by different screening mechanisms in these two measurements [34]. In XPS the initial ground-state valence electrons experience the full potential of an unscreened core hole, whereas in XAS the core electron can be excited into an efficient screening orbital so that the perturbation on the remaining ground-state electrons is small.

The $L_{2,3}$ XAS spectra can be analyzed to give information about the d-state occupancy. To address quantitatively the relationship between the white-line intensity and the number of d holes, we consider the sum of the areas in the white lines, which is expected to be proportional to the number of d holes in the unhybridized Co 3d band. To establish the numerical proportionality between the white-line intensity and the number of d holes, we follow the empirical method of Pearson, Ahn, and Fultz [35] for isolating and normalizing the white lines. Briefly, the background intensity was modeled by step functions in the threshold regions. A straight line over a range of 5 eV was fitted to the background intensity immediately following each white line. This line was then extrapolated into the threshold region and set to zero at energies below that of the white-line maximum. The areas in the white lines were added and then divided by the area in a normalization window 5 eV in width beginning 5 eV past the L_3 white-line onset. It needs to be pointed out that in 3d series the spin-orbit splitting of the edges is not large enough to prevent the mixing of the two white lines, which is caused by Coulomb interactions in the final states. This makes an exact separation of the two partners impossible; however, the effect becomes smaller than 5% for Co [36]. We also would like to point out that since the sample contains three phases, the experimental data are an average over different sites with different local coordinations. It is well known that the cohesive energy can be predicted from the filling of the d band, and a phenomenological relationship between the number of 3d holes per transition-metal atom (h_d) and the heat of formation (ΔH) was established recently for Ni_3Al [37]: $\Delta H = -[Ah_d(10-h_d)+B(10-h_d)]$, where A=-0.14 eV and B= 0.2 eV. We note that the measured number of 3d holes in elemental Ni is the muffin tin value of 1.4 instead of 0.6 expected for atomic d orbitals. If the h_d value of Ni_3Al (1.05) of Ref. [37] is used to scale that obtained by us [4], the h_d value for this Co-Al alloy is 0.7. If the above phenomenological relationship for Ni_3Al is used for this Co-Al alloy, the ΔH value for the latter is estimated to be -0.95 eV/atom. We note that our estimated ΔH value for Ni_3Al is -0.48 eV/atom [10], which is close to the experimental value of -0.43 eV/atom [38] and is exactly the same as that calculated by Xu, Oguchi, and Freeman [39] using an all-electron total energy local density approach. If one uses the h_d value of 0.9 for CoAl as proposed in Ref. [24], one would get the ΔH value of -0.68 eV/atom. This value is close to the experimental value of -0.56 ± 0.03 eV/atom [38]. Thus, the method used in this work is quite reliable in predicting the heat of formation for intermetallic compounds and alloys. Lastly, the branching ratio $I(L_3)/[I(L_2)+I(L_3)]$ for this Co-Al alloy

is 0.72, which is larger than the statistical value of 0.67. This observation indicates that this Co-Al alloy is a high-spin material [40].

CONCLUSIONS

The electronic structure of a Co-Al alloy was studied by four spectroscopic methods: XPS, BIS, RESPES, and XAS. The two-hole bound state is very weak in this Co-Al alloy, if it exists. Ferromagnetic exchange splitting of ~1.2 eV is obtained between the occupied spin-up and unoccupied spin-down states of this Co-Al alloy. The asymmetry index of the Co 2p core levels and thus the density of states at the Fermi level for this Co-Al alloy is larger than that for Ni_3Al and for CoGa. The number of 3d holes per Co atom is 0.7, and the heat of formation is estimated to be -0.95 eV/atom for this Co-Al alloy.

Acknowledgements-We thank J.-Y. Pieh and W.-F. Pong for the EDX measurement, and K.-L. Tsang and J. W. Allen for stimulating discussions. This work was supported by the National Science Council, Taiwan, R.O.C. through grants NSC 85-2112-M-018-006 and NSC 86-2613-M-018-001.

REFERENCES

Guillot, C., Ballu, Y., Paigne, J., Lecante, J., Jain, K. P., Thiry, P., Pinchaux, R., Petroff, Y., & Falicov, L. M. (1977), *Phys. Rev. Lett.* 39, 1632.

Davis, L. C. (1986), *J. Appl. Phys.* 59, R25, and references therein.

Allen, J. W. (1992), in *Synchrotron Radiation Research: Advances in Surface and Interface Science, Volume 1: Techniques*, edited by R. Z. Bachrach (Plenum Press, New York), and references therein.

Hsu, L.-S., Tsang, K.-L., & Chung, S.-C. (1996), *Mat. Res. Soc. Symp. Proc.* 437, 53.

Hsu, L.-S., Tsang, K.-L., & Chung, S.-C. (1998), *Intl. J. Mod. Phys.* B 12, 2757.

Hsu, L.-S., Gweon,G.-H.,& Allen, J. W. (1999), *J. Phys. Chem. Solids* 60, 1627.

Hsu, L.-S. & Williams,R. S. (1993), *Phys. Lett.* A 178, 192.

Hsu, L.-S. & Williams,R. S. (1994), *J. Phys. Chem. Solids* 55, 305.

Hsu, L.-S. (1995), *Phys. Rev.* B 52, 10858.

Hsu, L.-S., Tsang, K.-L., & Chung, S.-C. (1998), *J. Magn. Magn. Mater.* 177-181, 1031.

Weinelt, M., Nilsson, A., Magnuson, M., Wiell, T., Wassdahl, N., Karis, O., Fohlisch, A., Martensson, N., Stohr, J., & Samant, M. (1997), *Phys. Rev. Lett.* 78, 967, and references therein.

Lopez, M. F., Laubschat, C., Gutierrez, A., Hohr, A., Domke, M., Kaindl, G., & Abbate, M. (1994), *Z. Phys.* B 95, 9, and references therein.

Hsu, L.-S. (1998), *J. Phys. Chem. Solids* 59, 651.

Shen, Z.-X., Allen, J. W., Lindberg, P. A. P., Dessau, D. S., Wells, B. O., Borg, A., Ellis,W., Kang, J.-S., Oh, S.-J., Lindau, I., & Spicer, W. E. (1990), *Phys. Rev.* B 42, 1817; Kang, J.-S., Hong, J. H., Jeong, J. I., Choi, S. D., Yang, C. J. , Lee,Y. P., Olson, C. G., Min, B. I., & Allen, J. W. (1992), *Phys. Rev.* B 46, 15689; Kang, J.-S., Yang, C. J., Lee,Y. P., Olson, C. G., Cho, E.-J., Oh, S.-J., Anderson,R. O., Liu, L. Z., Park, J.-H., Allen, J. W., & Ellis,W. P. (1993), *Phys. Rev.* B 48, 10327.

Mitsuzuka, T., Kamijo, A., & Igarashi, H. (1990), *J. Appl. Phys.* 68, 1787; Kudryavtsev, Yu. V., Lee, Y. P., & Kim, K. W. (1998), *J. Appl. Phys.* 83, 1575.

Pearson, W. B. (1967), *A Handbook of Lattice Spacings and Structures of Metals and Alloys* (Pergamon Press, New York); Ellner, M., Kek, S., & Predel, B. (1992), *J. Alloys Comp.* 189, 245.

Hsu, L.-S., unpublished results.

Yeh, J.-J. & Lindau, I. (1985), *At. Data Nucl. Data Tables* 32, 1.

Polak, M., Deng, J., & Rubinovich, L. (1997), *Phys. Rev. Lett.* 78, 1058.

Himpsel, F. J. & Eastman, D. E. (1980), *Phys. Rev.* B 21, 3207; (1980), *Phys. Rev.* B 22, 5014.

Himpsel, F. J. & Fauster, Th. (1982), *Phys. Rev.* B 26, 2679.

Doniach, S. & Sunjic, M. (1970), *J. Phys.* C 3, 285.

Shirley, D. A. (1972), *Phys. Rev.* B 5, 4709.

Okochi, M. & Yagisawa, K. (1982), *J. Phys. Soc. Jpn.* 51, 1166.

Koch, J. M. & Koenig, C. (1986), *Phil. Mag.* B 54, 177.

Begot, J. J., Caudron, R., Faivre, P., & Costa, P. (1974), *J. Phys.* (Paris) 35, L125.

de Dood, W. & de Chatel, P. F. (1973), *J. Phys.* F 3, 1039.

Fletcher, G. C. (1972), *Physica* 62, 41.

Buis, N., Franse, J. J. M., & Brommer, P. E. (1981), *Physica* B 106, 1.

Ho, J. C., Liang, R. C. & Dandekar, D. P. (1986), *J. Appl. Phys.* 59, 1397.

Hufner, S. & Wertheim, G. K. (1975), *Phys. Lett.* 51A, 301.

Yin, L. I., Adler, I., Chen, M. H., & Crasemann, B. (1973), *Phys. Rev.* A 7, 897.

Richardson, D. & Hisscott, L. A. (1976), *J. Phys.* F 6, L127.

van der Laan, G., Zaanen, J., Sawatzky, G. A., Karnatak, R., & Esteva, J.-M. (1986), *Phys. Rev.* B 33, 4253.

Pearson, D. H., Ahn, C. C., & Fultz, B. (1993), *Phys. Rev.* B 47, 8471.

Carra, P., Thole, B. T., Altarelli, M., & Wang, X. (1993), *Phys. Rev. Lett.* 70, 694.

Muller, D. A., Subramanian, S., Batson, P. E., Sass, S. L., & Silcox, J. (1995), *Phys. Rev. Lett.* 75, 4744, and references therein.

Hultgren,R., Desai, P. D., Hawkins, D. T., Gleiser, M., & Kelley, K. K.(1973), *Selected Values of the Thermodynamic Properties of Binary Alloys* (American Society of Metals, Metals Park, OH).

Xu, J.-H., Oguchi, T., & Freeman, A. J. (1987), *Phys. Rev. B* 36, 4186.

Thole, B. T. & van der Laan,G. (1988), *Phys. Rev.* B 38, 3158.

收稿日期：90 年 06 月 14 日
修正日期：90 年 07 月 18 日
接受日期：90 年 08 月 15 日

Co-Al 合金的電子結構研究

*徐力行 鍾世俊 權奇洪
國立彰化師範大學物理系 同步輻射中心 美國密西根大學物理系

本文以高解析度 X 光光電子能譜、反光電子能譜、共振光電子能譜及 X 光吸收能譜來研究 Co-Al 合金的電子結構。此 Co-Al 合金之 Co 2p 內層能階的不對稱係數比 Ni_3Al 及 CoGa 為大。這現象表示此 Co-Al 合金之費米面的能態密度較 Ni_3Al 為大。由 X 光吸收能譜可知在此 Co-Al 合金中 Co 原子的 3d 電洞數為 0.7 。

關鍵詞：X 光光電子能譜　X 光吸收能譜　過渡金屬合金